

Visualization of Shock-vortex Interaction Radiating Acoustic Waves

Chang, S. M.*¹ and Chang, K. S.*²

*¹ School of Mechanical and Aerospace Engineering, College of Engineering, Seoul National University, San 56-1 Shinlim-dong, Kwanak-gu, Seoul 151-742, Korea.

*² Department of Aerospace Engineering, Korea Advanced Institute of Science and Technology, 373-1 Kusong-dong, Yusung-gu, Teajon 305-701, Korea.

Received 11 September 1999.

Revised 12 July 2000.

Abstract: Unsteady compressible flow fields past a wedge and a cone, evolved by propagation and interaction of shock waves, slip lines, and vortices, are studied by shadowgraphs and holographic interferograms taken during the shock tube experiment. The supplementary numerical calculation also presented time-accurate solution of the shock wave physics which was essential to recognize the similarity and dissimilarity between the wedge and the conical flows. The decelerated shock detained by the vortex interacts with the small vortexlets along the slip layer, producing diverging acoustics: this phenomenon is more distinct in the case of wedge flow for a given shock Mach number. The decelerated shock penetrated through the vortex core constitutes a transmitted shock, which eventually merges with the diaphragm shock that bridges the vortex pair/vortex ring. This phenomenon became remarkably salient in the case of conical flow.

Keywords: shock wave diffraction, holographic interferometry, shadowgraphy, computational fluid dynamics (CFD), shock tube experiment, acoustic waves, vortexlets.

1. Introduction

In the diffraction process, some shock waves are reflected either from the body surface or from the symmetric axis to make the interaction complex, even for a relatively simple body geometry. Dosanjh and Weeks (1965) visualized by Schlieren method and Mach-Zehnder interferometry a weak shock diffracted by a starting vortex. In their consecutive paper (Weeks and Dosanjh, 1967), they analyzed the acoustic radiation with Lighthill's formula and linearization approximation. Meadows et al. (1991) and Ellzey et al. (1995) investigated the shock-vortex interaction by adopting a perfect vortex model and numerically solving the Euler equations. However, the above two papers address an ideal case in which the quadrupolar acoustic waves are emitted by an isolated vortex intercepting a planar shock. The real shock-vortex interactions are far more sophisticated than what a model can present. Schardin's visualization with shadowgraphy (1957) of the shock diffraction behind a finite wedge, for example, shows unusually complex flow patterns. Sivier et al. (1992) numerically reproduced this experimental flow but computation was limited to a relatively early time. In the Schardin's experiment, a relatively narrow shock tube was used so that noise shock waves reflected from the upper and lower shock tube wall arrived at the test section to disturb the basic flow field prematurely.

The authors have improved this experiment in the present paper by using a relatively wider shock tube, of 150 mm × 60 mm test section size, to delay the arrival time of the noise shocks. Holographic interferometry and contact shadowgraphy are used for the experimental visualization. The Euler equations are simultaneously solved

on the quadrilateral unstructured adaptive grid with six levels of adatation, for numerical visualization of delicate weak waves. Test models are a finite wedge (namely, a triangular prism) for the two-dimensional flow and a finite cone for the axisymmetric case. The acoustic radiation by the shock-vortex interaction shall be clearly visualized on these two models.

2. Shock Wave Diffracted by a Finite Wedge

We first used a finite wedge: its cross section is an equilateral triangle with the side length 20mm long (Chang and Chang, 1999). Shock Mach number is $M_s = 1.34$, which is identical with that of the Schardin's experiment.

2.1 Comments on the Main Phenomena

The left side of Figs. 1(a)-(c) show the holographic interferograms, and the right is computational isopycnics or constant density contours. When the Mach stem (M_s) of the incident shock is diffracted around the vertex of the wedge, a starting vortex (V) is produced. The slip line (S_i) from the triple point (T_i) is hurled around the vortex in the clockwise direction, part of which is overlapped with the so-called entropy layer. The reflected shock (R_i) of M_s also runs into the vortex. The clockwise rotation of V accelerates that part of R_i between the vortex and the wedge wall into a fast-moving circular wave (A), and decelerates the rest of R_i by detaining its one end at the vortex center (D). Time up to the appearance of this A and D waves shall be called the early stage of shock-vortex interaction in this paper.

Figures 2(a)-(d) show detailed wave structure in the later stage of the shock-vortex interaction. We can observe from the left shadowgraphs some secondary waves which are much weaker than the shock waves. Shown on the right are the schematic drawings and magnified view of computational results for the phenomenon presented on the left.

2.2 Diverging Acoustics and Transmitted Shock

The shadowgraphs in Figs. 2(a)-(d) clearly visualize the slip layer from the wedge vertex, degenerated into the vortexlets due to the Kelvin-Helmholtz instability. The vortexlets constitute periodic density variation on the vortex edge which interact with the decelerated shock (D) which is in counterclockwise progression. The shock-vortexlet interaction results in emission of weak compressive waves called diverging acoustics D_1, D_2, \dots , all emerging from a single source point on the shock wave D . They are the envelopes of the acoustic waves radiated from the vortexlets. Computational results also show these diverging acoustics.

In the interior of the primary vortex (V), the shock D penetrates the vortex core to appear as a transmitted shock (TS). The two transmitted shocks emitted from V and its mirror vortex (V') are connected eventually to form what we call a diaphragm shock; see Figs. 2(c)-(d).

3. Shock Wave Diffracted by a Finite Cone

We also performed an experiment and computation for a finite cone having the same cross-sectional shape in the meridional plane. Two shock Mach numbers are chosen, $M_s = 1.34$ and 1.73 , to see the influence of shock strength.

3.1 Comments on the Conical Problem

Sight integration effect in the interferogram prevents comparing the computational results directly with the experimental photographs for an axisymmetric problem (Mayinger, 1994). The new concept of light-path averaged density is proposed in this paper to make the direct comparison possible. We define $\bar{\rho}$, the light-path averaged density, by setting $\bar{y} = \sqrt{x^2 + y^2}$, as follows:

$$\begin{aligned}\bar{\rho}(x, y) &= \frac{2}{d} \int_0^{d/2} \rho(x, \bar{y}) dz \\ &= \frac{2}{\sqrt{R^2 - y^2}} \int_y^R \rho(x, \bar{y}) d\sqrt{\bar{y}^2 - y^2}\end{aligned}\quad (1)$$

where the symbols and notations are explained in Figs. 3(a)-(b). Suppose the density distribution ρ is known on the meridional cross-section. Then the new property $\bar{\rho}$ calculated by Eq. (1) can be expressed in the following form

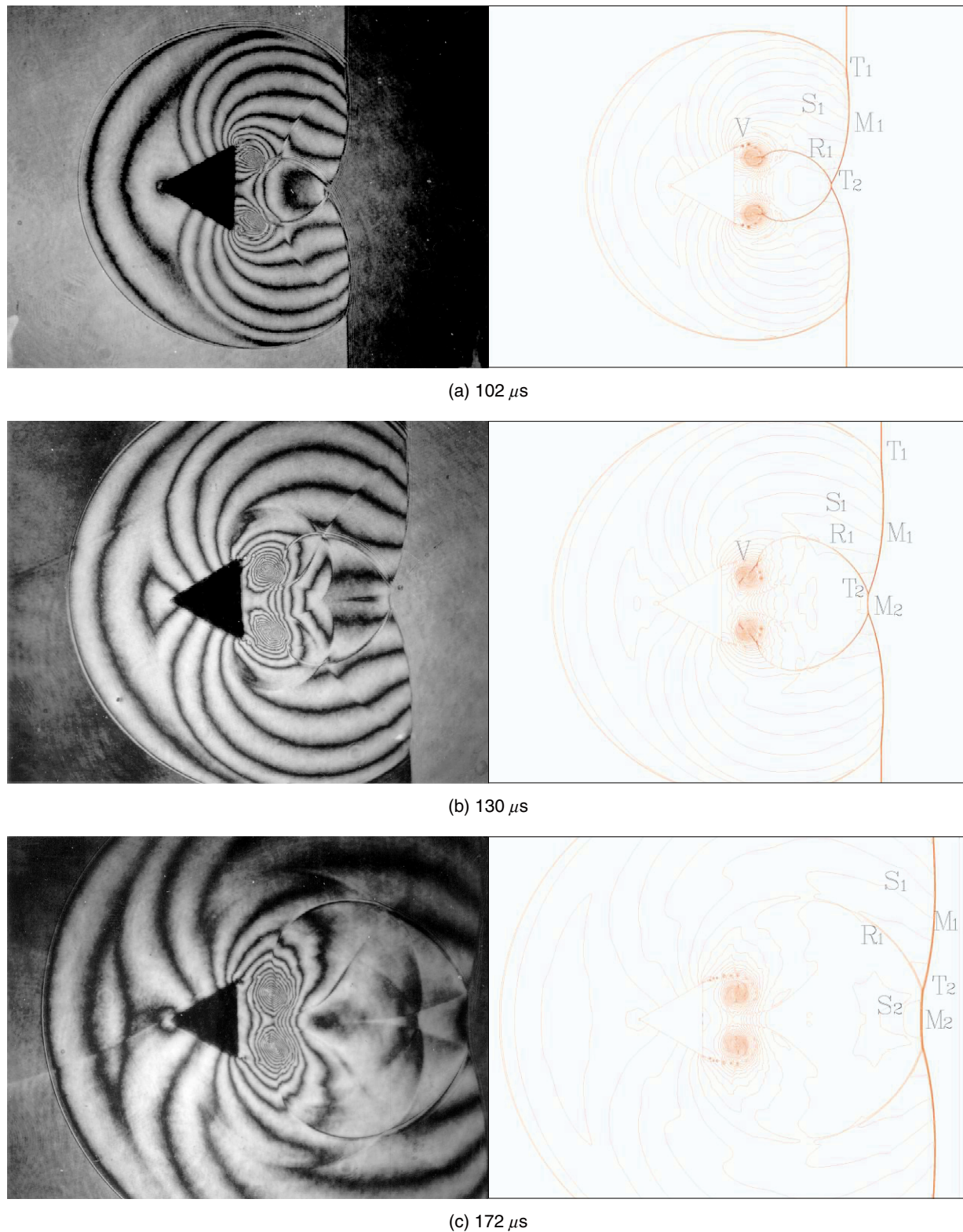


Fig. 1. Shock diffraction by a finite wedge, $M_s = 1.34$: Experimental interferograms (left) and computational isopycnics (right).

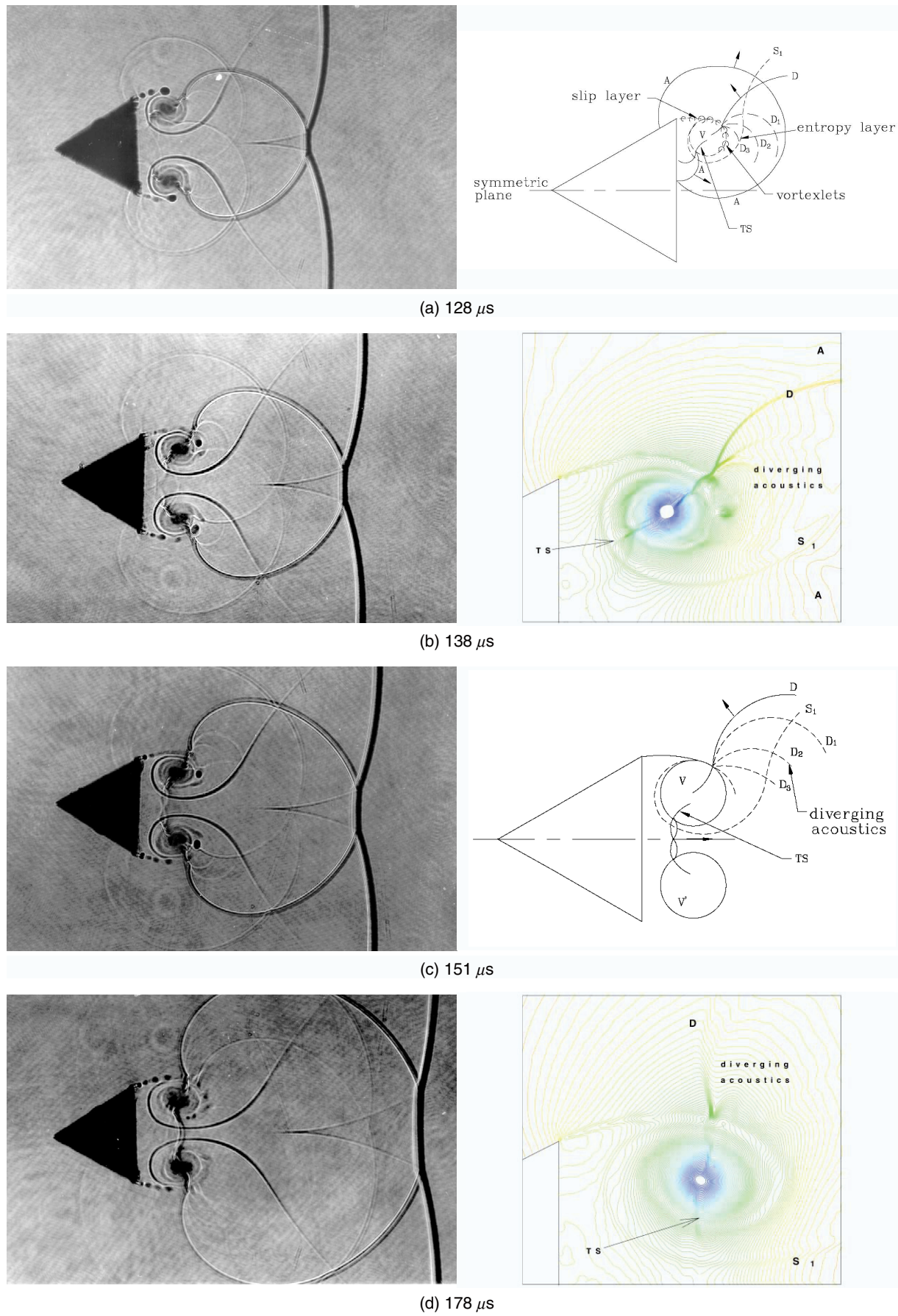


Fig. 2. Shock diffraction by a finite wedge, $M_s = 1.34$: Left: shadowgraphs, right (a), (c): schematic diagrams, right (b), (d): magnified view of numerical results.

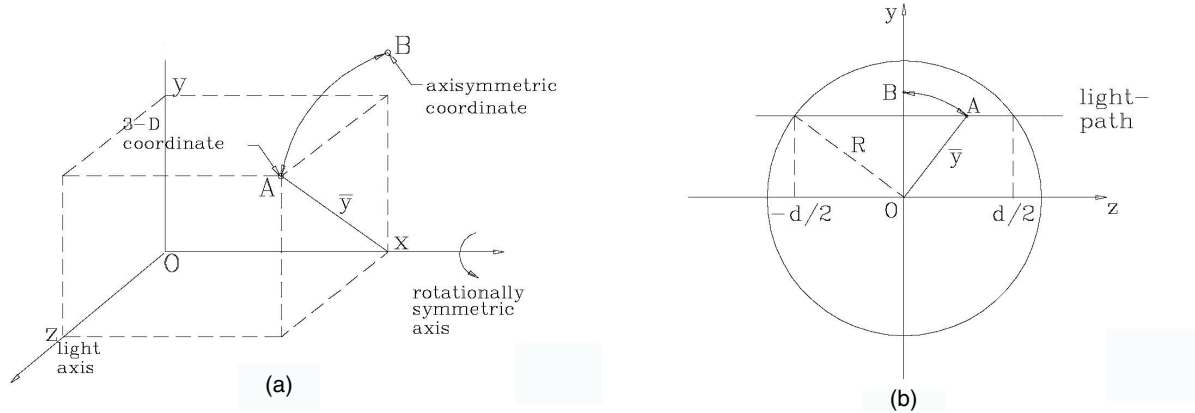


Fig. 3. Mapping between two coordinate systems: $A(x, y, z)$ in three dimension is equivalent to $B(x, \bar{y})$ in axisymmetric plane.

derived from the Gladstone-Dale equation valid for the low density gases,

$$\Delta\bar{\rho} = \frac{\lambda}{Kd} \quad (2)$$

where λ is the wavelength of light, and K is a proportional constant. Therefore the $\bar{\rho}$ field can now be compared with the interferogram in the axisymmetric flows, similarly to the two-dimensional problems.

The left of Figs. 4(a)-(d) is experimental interferograms whereas the right is computational isopycnics (lower half) plus the numerical interferogram obtained by Eq. (2) (upper half). The main phenomenon does resemble shock diffraction over a wedge, but the present axisymmetric interaction is much weaker because both the shock wave and the vortex have lower strengths due to the three-dimensional relieving effect. We can notice that the interaction of D and V for the case of $M_s = 1.73$ in Fig. 4(d) is much stronger than the case of $M_s = 1.34$ in Fig. 4(b).

3.2 Transmitted Shock and Diaphragm Shock

Figures 5(a)-(d) are the computational results, showing details of the wave pattern including the secondary wave components. Like the two-dimensional cases, diverging acoustics (DA) and transmitted shock (TS) are observed. Shape of the vortexlets along the vortex ring is not as distinct as the wedge problem, but we can discern some DA's in Figs. 5(a)-(c).

A notable difference is observed, however, in the transmitted shock of Figs. 5(b)-(c). The so-called diaphragm shock (DS) (Chang and Kim, 1995) that appears like a diaphragm covering the vortex ring is formed in the compression region at the base of the cone; see Fig. 5(b). DS plays the role of compressing the rotating flow entrained in the base of the cone (Hiller, 1991). TS catches with DS to merge into one; see Fig. 5(c). Figure 5(d) is the schematic diagram of Fig. 5(b).

4. Conclusion

Time-accurate experiment and computer simulation have been conducted to analyze the shock-vortex interaction past a wedge and a cone. Holographic interferometry serves to reveal the entire flow field. Shadowgraphy provides information on the strength and location of the shock or compressive waves. Computational results can offer sampling of the flow fields during the time-dependent simulation as frequently as one wants. They are complementary with each other in building a complete picture of the phenomena.

The primary interest of this paper is focused on visualizing the shock-vortex interaction radiating acoustic waves. The impinging shock wave is split into the decelerated and accelerated shocks by the vortex. The decelerated shock radiates acoustic waves as it interacts with the vortexlets produced by shear layer instability; the diverging acoustics radiated from one source point are much curved in the form of circular arcs by the external rotating flow. The transmitted shock is merged with the diaphragm shock that bridges the separated vortices. In

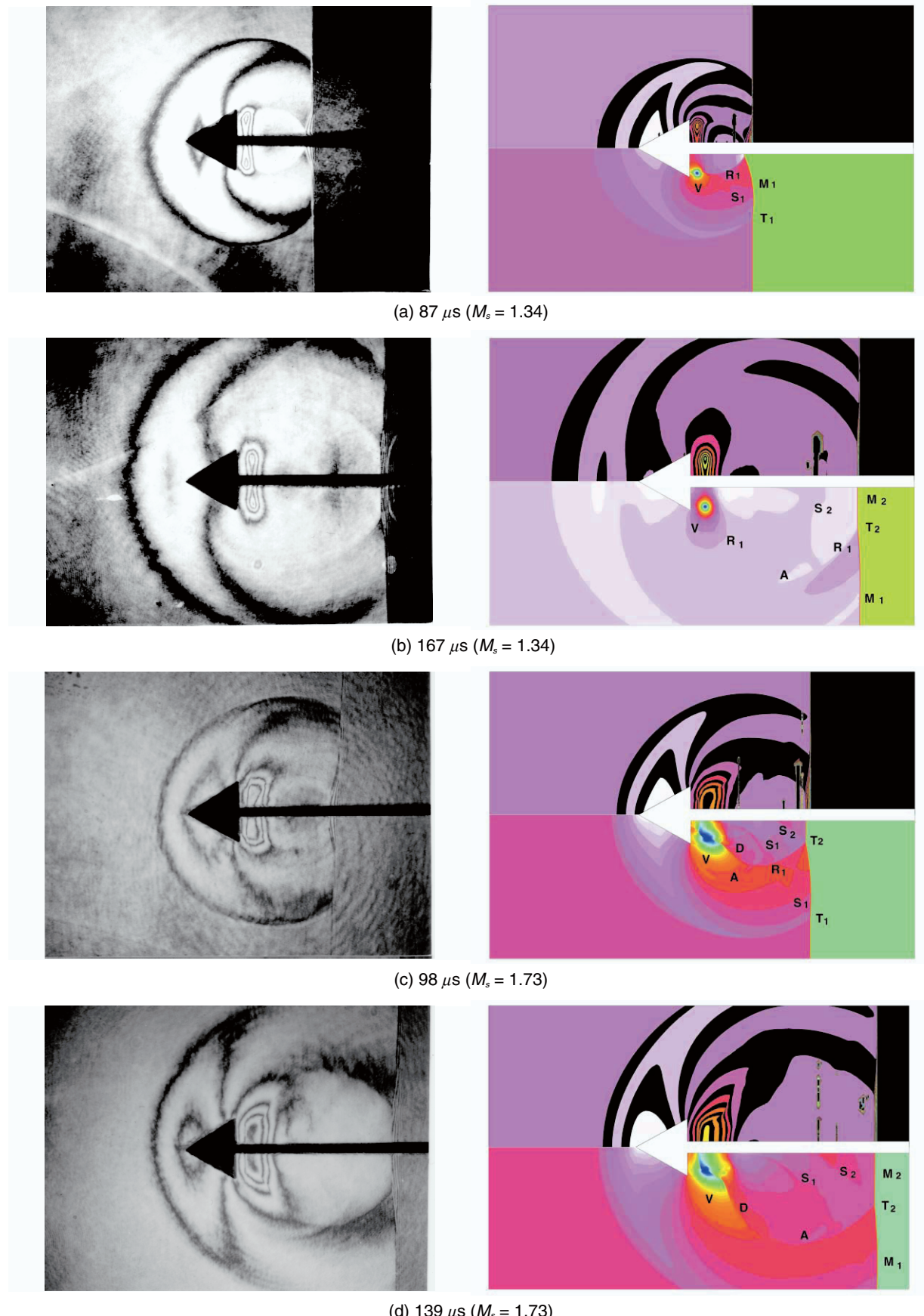


Fig. 4. Shock diffraction by a finite cone: Experimental interferograms (left); computational isopycnics (right lower half); numerical interferograms (right upper half).

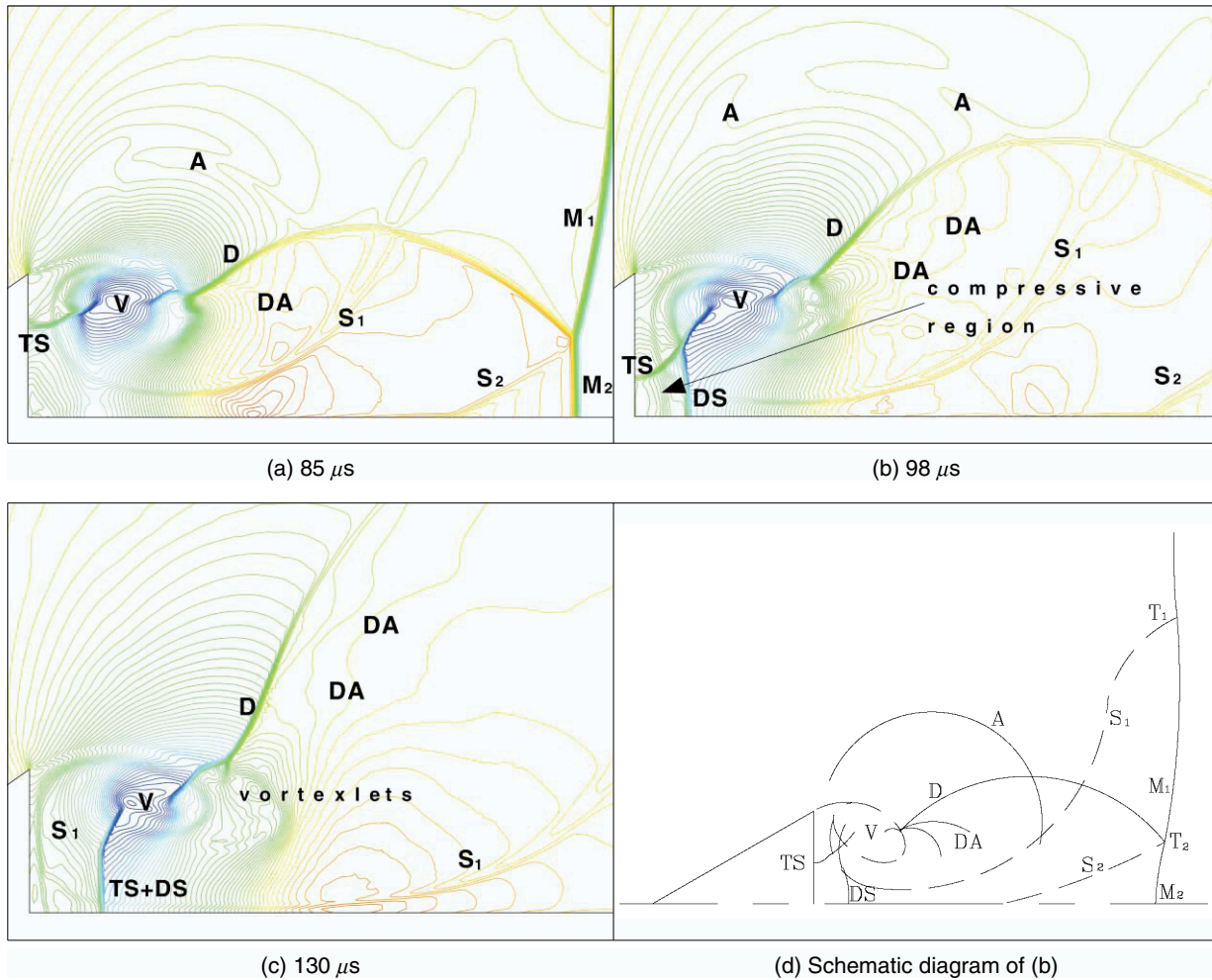


Fig. 5. Shock diffraction by a finite cone, $M_s = 1.73$: Magnified view of numerical results.

the wedge flow, the diverging acoustics were distinctive because of the relatively strong interaction between the decelerated shock and the vortexlets. For the conical flow, the merged transmitted shock and diaphragm shock became relatively strong due to the axisymmetric compression of the base flow by the vortex ring.

References

- Chang, K. S. and Kim, J. K., Numerical Investigation of Inviscid Shock Wave Dynamics in an Expansion Tube, *Shock Waves*, 5 (1995), 33-45.
- Chang, S. M. and Chang, K. S., Shock Wave Scattering Phenomena Behind a Finite Wedge, Proceeding of 5th Asian Symposium of Visualization 1998(Puspittek Serpong, Indonesia), (1999-3), 47-52.
- Dosanjh, D. S. and Weeks, T. M., Interaction of a Starting Vortex as well as a Vortex Street with a Travelling Shock Wave, *AIAA*, 3 (1965), 216-223.
- Ellzey, J. L., Henneke, M. R. and Picone, J. M. and Oran, E. S., The Interaction of a Shock with a Vortex: Shock Distortion and the Production of Acoustic Waves, *Physics of Fluids*, 7 (1995), 172-184.
- Hiller, R., Computation of Shock Wave Diffraction at a Ninety Degree Convex Edge, *Shock Waves*, 1 (1991), 135-144.
- Mayinger, F., Fundamentals of Holography and Holographic Interferometry in Optical Measurement - Techniques and Applications (Editor: Mayinger, F.), (1994), 51-73, Springer-Verlag.
- Meadows, K. R., Kumar, A. and Hussaini, M. Y., Computational Study on the Interaction Between a Vortex and a Shock Wave, *AIAA*, 29 (1991), 174-179.
- Schardin, H., High Frequency Cinematography in the Shock Tube, *Journal of Photo Science*, 5 (1957), 19-26; see also Van Dyke, *An Album of Fluid Motion*, (1982), Parabolic Press, Stanford, California.
- Sivier, S., Loth, E., Baum, J. and Lohner, R., Vorticity Produced by Shock Wave Diffraction, *Shock Waves*, 2 (1992), 31-41.
- Weeks, T. M. and Dosanjh, D. S., Sound Generation by Shock-Vortex Interaction, *AIAA*, 5 (1967), 660-669.

Author Profile

Se-Myong Chang: He earned his Ph.D. degree from Korea Advanced Institute of Science and Technology (KAIST) in 2000 under the supervision of Prof. Keun-Shik Chang. He now works as Brain-Korea-21 Post-doctoral Fellow at Seoul National University. His research fields are shock-vortex interaction, computational aero-acoustics and experiment of high-speed flow.



Keun-Shik Chang: He finished his academic discipline of Ph.D. at the University of California, Berkeley in 1977, and NRC Research Associateship at NASA-Ames Research Center in 1978. He has since served as a professor of Department of Aerospace Engineering in Korea Advanced Institute of Science and Technology (KAIST). He is the founder of Korean Society of Computational Fluids Engineering (KSCFE). His research interests are in engineering flow computation and shock wave experiment. He has published hundredsome international journal and conference papers.